

A Statistical Framework for Performance Analysis of Diversity Framed Slotted Aloha with Interference Cancellation

Pietro Cassar, Tomaso de Cola, *Member, IEEE*, and Alberto Gotta

Abstract

As the Internet of Things (IoT)/Machine-to-Machine (M2M) market is rapidly growing, a special role is expected to be played by satellite communications in that they offer ubiquitous coverage and therefore enable typical monitoring, telemetry, and control services also in areas with a poor terrestrial infrastructure. In this respect, the case of massive IoT devices deployment calls for random access solutions, which have been long analysed by the scientific satellite community in the last ten years. This paper further elaborates on the relation between the normalised offered load and the achievable performance in terms of packet loss rate, which was not much addressed so far at high loads. The proposed theoretical framework has been validated through extensive simulation campaigns, which show an excellent match at different loads and number of interfering packets configurations, by significantly improving the results achievable through other existing theoretical frameworks.

Index Terms

Maritime SatCom, M2M, D-FSA, IC, Random Access.

I. INTRODUCTION

The IoT/M2M market has been tremendously growing over the last years, because of the compelling need to digitalise industry factories so as to develop the *Industry 4.0* concept as well

P. Cassar and A. Gotta are with the National Research Council, Institute of Information Science and Technologies, Pisa, PI, 56124 Italy e-mails: alberto.gotta@isti.cnr.it, pietro.cassara@isti.cnr.it.

Tomaso De Cola is with the Deutsches Zentrum fur Luft- und Raumfahrt e.V., German Aerospace Center Institute of Communications and Navigation, Wessling, 82234 Germany e-mail: Tomaso.deCola@dlr.de

Manuscript received November xx, 2019; revised ...

as to provide command and control means to general assets. As a matter of fact, this is not just limited to the case of industry “robotisation” or energy plant monitoring but also addresses remote properties and assets, such a ship and cargo tracking, precision-agriculture, and overall comprehends small data sectors. Particularly interesting is the case of IoT services to be offered in remote areas, which is becoming an attractive market with an ever-increasing growth of the overall return-of-investment and with a consequent increase of the number of services and IoT devices being deployed [1].

In this context, particularly appealing is the use of satellite communications, thanks to the ubiquitous coverage and the recent advances in satellite antenna miniaturisation so that IoT devices enabled to data communication through satellite are becoming a non-expensive attractive option [2]. Moreover, the sectors, where the terrestrial infrastructure is not available or in any case the offered network capacity cannot sustain the traffic generated by massive IoT deployment certainly make the satellite the only viable solution. This trend is more importantly confirmed by the interest raised in the 5G standardisation task carried out within 3GPP with respect to the use cases of massive Machine-Type Communications (mMTC) [3]. In particular, the defined Non Terrestrial Network (NTN) work item entails also the case of direct access from new-radio (NR) devices directly to satellite [4], which is well representative of IoT over satellite use cases. In this respect, different satellite systems are being considered as potential technology candidates to enable these services. On the one hand, Geosynchronous (GEO) satellites are often considered as a proper solution, because of the large coverage with a single satellite and thanks to well-defined standards as well as consolidated experience in this field from many satellite vendors and operators. On the other hand, Medium-Earth Orbit (MEO) constellations have been receiving more and more consensus as they offer similar performance of GEO but a lower service delay and necessitate only few satellite platforms more. Finally, the renewed interest towards Low-Earth Orbit (LEO) systems and in particular the plan and the launch of *mega-constellations* (composed of hundreds/thousands satellite platforms) can further boost the market of IoT over satellite.

Independently of the specific satellite systems being considered, one of main design challenges to be faced is represented by the dense deployment of sensor nodes, which may need to access the satellite capacity simultaneously. As such, the problem of media access control is pivotal for achieving efficient data communication. In this respect, it is immediate to see that dedicated-access schemes cannot be considered a viable solution because of the bursty nature of the IoT

traffic, which could cause a waste of the allocated satellite resources and ultimately lead satellite operators to reject the allocation requests from many of the IoT devices. On the contrary, the profitability of random access schemes is certainly much more appealing, also thanks to the evolution of the old *ALOHA* (in asynchronous and slotted mode) concept. To this regard, the scientific community has carried out important studies in the last ten years, aimed at finding out the best strategy to access the satellite capacity, by taking into account the available degrees of freedom to be exploited. In more details, some of the most important research lines have related to the use of multiple replicas so as to achieve time diversity transmission as well as Interference Cancellation (IC) implemented at the receiver side, in order to recover from slot collisions occurring especially in the case of moderate and high network traffic loads. Investigations have considered the cases of both slotted and un-slotted access, in order to analyse the achievable performance also in relation to the induced implementation complexity in real devices.

More specifically, the scientific community has elaborated several schemes in the last years [5], [6], by taking the consolidated Slotted ALOHA (SA) and Framed Slotted ALOHA (FSA) schemes as baseline and extending them with novel concepts such as time diversity (e.g. in Diversity - Framed Slotted ALOHA (D-FSA) [7]) and IC, the latter being exploited in many proposals such as Contention Resolution Diversity Slotted ALOHA (CRDSA) [8], Irregular Repetition Slotted ALOHA (IRSA) [9], and Coded Slotted ALOHA (CSA) [10]. In more detail, FSA and D-FSA schemes may introduce significant number of packet losses or even cause undesirable service unavailability. On the other hand, a great performance improvement, in terms of throughput, comes from applying IC to D-FSA. In this case, the replicas transmitted within a Media Access Control (MAC) frame keep a pointer to the twin slots: whenever a clean burst is detected and successfully decoded, the potential interference contribution caused by the twin replica is cancelled in the pointed slot, hence resulting in a remarkable throughput improvement with respect to SA. A further improvement may be achieved either by increasing the number of replicas to k , either letting k be a random variable sorted by a discrete distribution [9], or being k the coded fragments of a packet of m bits, with $m < k b$, and b being the size [bits] of a time slot [10].

The vast literature available so far was mostly focused on asymptotic limits or, in any case, the developed mathematical frameworks were not able to properly investigate the impact of the number of IoT devices on the overall performance [11] and, to the best of authors' knowledge, none of the existing studies is able to provide a complete statistical characterization of the system.

In fact, when an RA system undergoes a variable traffic load (as for instance with sporadic and unpredictable M2M traffic), so that the system cannot be considered in steady state, then first- and second-order statistics are not sufficient to characterize the performance of the system. On the contrary, knowledge of the probability distribution of the number of collided users would help in carrying out a more thorough performance analysis, which is an important scientific problem not completely solved by the literature, to the best of the authors' knowledge.

To this aim, this paper extends and improves the analytical framework presented in [12] to calculate both the distribution of the number colliding users and the average number of colliding packets per time slot in each frame of a D-FSA satellite-based system. More interestingly, the proposed framework shows important theory findings able to close the gap between the results obtained from realistic simulations and those coming from the existing theoretical frameworks. This aspect is particularly remarkable at moderate/high load, where the existing frameworks typically provide weak approximations, whereas the one proposed in this paper is able to offer far better results.

The remainder of this paper is structured as follows. The theoretical framework is described in Section II. Validation of the theoretical findings through a simulation campaign in a significant use case is in Section III, whereas final conclusions and considerations are drawn in Section IV.

II. THEORETICAL FRAMEWORK

A. Loop Model

As presented in the introduction, IC is able to solve collisions throughout an iterative process if at least one replica of a packet can be correctly decoded. This means that the replica is alone in a time slot or takes advantage of the capture effect in case of unbalanced powers at the receiver. Otherwise, all the replicas of a user collide in a frame, incurring in a loop, by definition. Let us introduce the fundamental loop concept, which we use in what follows to characterize both D-FSA and the contention resolution in all the recent RA variants with IC. A *loop* occurs when two or more users send their replicas in the same time slot(s). For the sake of clarity, we provide just few examples. Two users u_1 and u_2 with two replicas each ($k = 2$) collide - in case of perfect power balancing - if they transmit the replicas in the same two time slots t_1, t_2 out on n time slots in a frame. Let's say that u_1 and u_1 have $v = 2$ intersections. With $k > 2$, again, the two users share the same k -tuples in the case of loop, giving $v = k$ intersections over the

time slots $t_1 \dots t_k$ out of n . Three users u_1, u_2 , and u_3 with 2 replicas each still share the same 2-tuple. However, with $k = 3$, two possible events may occur, given a loop:

- 1) u_1, u_2 , and u_3 share the same 3-tuples leading to 3 intersections over 3 time slots out of n ;
- 2) u_1, u_2 , and u_3 sort different 3-tuples but leading to 2 intersections over 4 time slots out of n .

The second case is shown by means of an example in Table I: the x symbol represents a replica of the users $u_1 ; u_2 ; u_3$ belonging to the loop, and the pool of four time slots L_l is $\{t_1 ; t_2 ; t_3 ; t_4\}$. Instead, the o symbol in Table I represents a replica transmitted by a user non in loop, i.e., with at least a replica in a time slot with no other packets, as in $(u_4 \text{ at } t_6, u_5 \text{ at } t_7)$. Note that, the users $u_1 ; u_2 ; u_3$ are in loop regardless of other users.

TABLE I: Example of the pool of time slots involved in a loop with $l = 2$ users.

| | t_1 | t_2 | t_3 | t_4 | t_5 | t_6 | t_7 |
|-------|-------|-------|-------|-------|-------|-------|-------|
| u_1 | x | | x | x | | | |
| u_2 | x | x | x | | | | |
| u_3 | x | x | | x | | | |
| u_4 | o | | o | | | | o |
| u_5 | o | | | o | | | o |

More generally, an l -order loop is given by $l+1$ users with $l-1$ ¹, which have chosen exactly the same pool L of time slots to send their replicas and all the time slots $t_j \in L$ are affected by a collision generated *at least*² by the $l+1$ users. Loops cause a contention between users that can be very hard to be decoded, unless other mechanisms are in place, i.e., when coding techniques are applied or when power imbalance between users occurs, thus giving rise to the *capture effect*. Not only, loops are one of the main reasons for Packet Loss Rate (PLR) due to unresolved collisions via IC.

¹The case $l = 0$ means that there is no loop.

²In fact, the other $l-1$ users can transmit at most $k-1$ replica on L in order to not belonging to the loop.

The loop probability in the first case, in which all the collided users share exactly the same time slots, has been investigated in [13]. Loops are one of the main reasons for packet losses, measured by means of PLR. In D-FSA, each user selects a set of k distinct time slots from a set of n elements in a MAC frame. Then, the user can choose any of the possible combinations with an equal probability $q = \frac{k}{n} \binom{n}{k}^{-1}$. Consider now a generic packet of interest (PoI). The probability that a user, attempting a PoI, is in a loop with l other users follows the binomial distribution, as in [13]:

$$B_L(u-1; q) = \binom{u-1}{l} q^l (1-q)^{u-1-l}; \quad (1)$$

with u the number of users per frame.

However, Eq. (1) in [13] does not accurately model the statistical occurrence of loops. In fact, (1) accounts for the probability that l users select the same tuple of replicas of the PoI and that the other $u-l$ ones not. However, this condition does not guarantee the other $u-l$ users to avoid creating a loop themselves. Yet, (1) accounts for a particular loop event, i.e., the loop takes only k time slots. This is highly probable only when $l = 1$.

Since Eq. (1) is not suitable to precisely characterise a loop event, let's introduce $P_{loop}(l)$ defined as:

$$P_{loop}(l) = (l; u; n; k); \quad (2)$$

that accounts for the probability that l users are in a loop with a PoI with their k replicas, over a subset of time slots out of n , and $u-l$ users must not belong to the loop. This condition guarantees that the $u-l$ users will successfully take advantage of interference cancellation, actually being removed from the contention on the current frame. Accordingly, it is possible to derive a more precise analytical expression for $(l; u; n; k)$ which is discussed in the Appendix, where also the novel mathematical framework applied in this work is illustrated.

B. Contention Resolution and Interference Cancellation

Let $(E_b=N_0)$ be the function that describes the packet error rate for a given channel code and modulation scheme, as characterized in [13], [14], as well. The loss probability ϵ for a

packet incurring in a loop with other l interfering packets is defined in [12] for an Additive White Gaussian Noise (AWGN) channel as:

$$P_l = \prod_{i=1}^l \frac{1}{k} 10 \log_{10} \frac{E_b=N_0}{1 + \prod_{j=1}^i (E_b=N_0)_j} \frac{1}{r \log_2 M} f_{l|L}(ij|l); \quad (3)$$

with coding rate r , M symbols, and $f_{l|L}$ being the probability of having i interfering packets of the set L_l of the loop with a packet in a PoI of l -order. From [9], the probability that a user attempts a PoI is equal to $p_t = \frac{k}{n}$ and the probability that the PoI node has *degree* i out of l from the bipartite graph theory is given by the binomial distribution $B_l(l; p_t)$. However, the condition of being in loop imposes excluding the probability of having less than two packets in a PoI. Therefore, $f_{l|L}(ij|l)$ can be derived as the truncated distribution $B_{l;trunc}(l; p_t)$ over the domain interval $(1; l]$ according to:

$$f_{X;trunc}(x) = \frac{f_X(x)}{F_X(x_{max}) - F_X(x_{min})}; \quad (4)$$

with PMF f_X and CDF F_X , respectively, over the domain $(x_{min}; x_{max})$.

The IC process aims at reducing the degree l of a loop, by performing iterative cancellations of packets correctly decoded in other time slots. Yet, in the case of spread spectrum techniques, $(E_b=N_0)_j$ in (3) must be divided by the spreading factor Sf , as shown in [14].

Finally, the probability that a PoI remains in a loop of degree l with $l = 1; 2; \dots; U - 1$ users (after IC) equals considering a generic user out of $l + 1$ to be in loop and it comes from Eqs. (2) and (3) as:

$$PLR = \frac{1}{U} \prod_{l=1}^{U-1} (l+1) P_{loop}(l); \quad (5)$$

C. Multi User Interference Distribution Function

In order to account for more general conditions than an AWGN channel, we assume the presence of possible multipath fading or shadowing effects. We assume that the spatial distribution of concurrently transmitting users follows a deterministic general model, i.e., a finite number of users are within a finite region and they transmit with the same level of $E_b=N_0$ [dB]. Under these assumptions, we provide a solution for the Probability Density Function (PDF) of the interference generated by l colliding packets with a PoI, by exploiting the theories of

stochastic geometry applied to the wireless networks [15], [16]. The interference generated by i packets in a time slot is:

$$I = \sum_{j=1}^{\infty} B_j \left(\frac{k}{n} \right)^{\alpha} \frac{E_b}{N_0} \quad (6)$$

where j is the index relative to the j -interfering-packet with Signal-to-Noise Ratio (SNR) of $\left(\frac{E_b}{N_0} \right)_j$ and $B_j \left(\frac{k}{n} \right)^{\alpha}$ the distribution from (4). In [17] expressions for the PDF of the interference power in a network whose transmitters are arranged according to the Poisson Point Process (PPP) are derived. Authors show that for a generic distribution $f_G(g)$ of the fading power, the resultant PDF $f_I(i)$ of the interference I can be obtained by numerical techniques. Precisely, they show some results of the inversion of the Laplace's transform of the interference power $L_I(s) = \exp \left\{ -\int_0^{\infty} \int_0^{\infty} \lambda^2 s^2 g \right\}$ where λ is the density of the transmitters, $\Gamma(\cdot)$ is the Gamma function, $E[\cdot]$ represents the expectation of its argument, α is the path loss exponent, assuming that the fading value g is distributed according to distributions such as Rayleigh, Nakagami- m , and Rice. Note that, when $f_G(g)$ is Nakagami- m distributed, a direct expression of the Signal to Noise plus Interference Ratio (SNIR) distribution $f_{JI}(j, I)$ is calculated in [18] for both the cases, when the signal of interest (W) and the interfering signal (I) have different Nakagami- m distributions ($m_I \neq m_W$) and when $m_I = m_W$, respectively. The SNIR is written as the ratio of two variables $U = \frac{E_b}{N_0} W$ and $V = 1 + \frac{E_b}{N_0} I$, respectively, whose distributions are:

$$f_U(u) = \frac{f_W \left(\frac{u}{\frac{E_b}{N_0}} \right)}{\frac{E_b}{N_0}} \quad \text{and} \quad f_V(v) = \frac{f_I \left(\frac{v-1}{\frac{E_b}{N_0}} \right)}{\frac{E_b}{N_0}}$$

respectively.

Calculating the quotient distribution of two random variables, the PDF for the SNIR $f_{JI}(j, I)$ at the receiver is given, numerically, in [18]. Rayleigh and Rician fading are particular cases of Nakagami- m fading with $m = 1$ and $m = \frac{(\kappa+1)^2}{2(\kappa+1)}$, respectively, being κ the Rice's factor, i.e., the ratio of the signal power in the dominant Line of Sight (LOS)-component to the power of other non-LOS components. Therefore, Eq. (3) can be generally written as:

$$f_{JI}(j, I) = \sum_{i=1}^{\infty} \lambda^k (E[\cdot])^k f_{IJL}(ij, I) \quad (7)$$

where $E[\cdot] = \int_0^{\infty} f_{JI}(j, I) dI$.

III. PERFORMANCE EVALUATION

For the performance evaluation, we selected an application scenario to be particularly attractive for IoT services over satellite systems. To this aim, a satellite system for data maritime communications among vessels operating far from harbours has been chosen as reference scenario. In fact, GEO systems for maritime communications are recently becoming more attractive than LEO systems, due to the larger data traffic injected into satellite systems, as a consequence of the data-traffic increment over oceans. Moreover, some of the main GEO satellite operators have extended their business towards satellite-on-the move systems, hence naturally embracing additional maritime data services (e.g. Inmarsat).

The reference scenario assume a satellite system operated in Ka frequency band, so as to enable highly reliable and timely M2M services, in terms of monitoring and control of vessel activities over vast coverage areas with users in mobility, whilst guaranteeing the needed data rate for real-time communications of diverse sensors and actuators displaced on vessels.

A. Channel Model

The characterization of the maritime satellite channel has been largely investigated [19]–[24] since the past decades. According to the conducted measurement campaigns and the corresponding channel models in [19], we assume in this work that the envelope of the signal received by the mobile terminal follows the Rice distribution, which describes the terminal-satellite communications in Line of Sight (LoS), to which additional distorted signal replicas are summed up, to account for signal reflections caused by the water surface. In more detail, the Rice factor, characterizing the received power distribution of probability, depends on the elevation angle: by taking into account that the received power due to LoS communication increases with the elevation angle, the Rice factor increases as well. The delay, incurred between the reception of the LoS path signal and the multi-path components, falls within hundreds of nanoseconds. On the other hand, the impulse channel response exhibits a number of echoes that can be assumed as Poisson-distributed with rate between 1 and 2 echoes within the RMS delay spread τ_{RMS} , as in the case of open space communications, indicating a rapid decay of the impulse channel response. An extensive simulation campaign has been conducted on the Satellite Network Simulator (S-NS3) simulator [25]. In S-NS3, the system allocates 2 GHz to the feeder link from 17.7 GHz to 19.7 GHz for the downlink and 500 MHz to the user link from 29.5 GHz to 30 GHz for the uplink: the link budget for Ka-band system under investigation is provided, according to the Digital

TABLE II: Simulator set-up parameters

| Name | Value |
|---------------------------|------------------|
| Random Access (RA) scheme | 2- 3-CRDSA |
| RA blocks per superframe | 1 |
| RA block duration | 13 [ms] |
| Timeslots per RA block | 64 |
| DVB-RCS2 Waveform Id | 14 |
| Mapping Scheme | QPSK |
| Code Rate | 1/2 |
| Burst Length | 202 [B] |
| Payload Length | 188 [B] |
| Gross bandwidth | 12.5 [MHz] |
| Symbol rate | 8.01 [Msymbol/s] |
| Roll off | 0.2 |
| Carrier spacing | 0.3 |
| One-way PHY delay | 0.13 [s] |

TABLE III: Link budget parameters in S-NS3

| S-NS3 Parameter | User Terminal | GEO Satellite | Gateway |
|------------------------|---------------|---------------|---------|
| txMaxPower [dBW] | 4 | 15 | 8.97 |
| txAntennaLoss [dB] | 1 | 1 | 0 |
| rxAntennaLoss [dB] | 0 | 1 | 0 |
| noiseTemperature [dBK] | 24.6 | 28.4 | 24.6 |
| txMaxAntennaGain [dB] | 45.2 | 54 | 65.2 |
| rxMaxAntennaGain [dB] | 44.6 | 54 | 61.5 |

Video Broadcasting - Return Channel via Satellite (DVB-RCS2) specification, in [26]. Table II provides all the parameters³ used to set up the simulator while default values of the link budget are provided in Table III. A custom channel model has been developed in S-NS3, in order to account for a satellite maritime with fading. By using the measurements of the direct-to-multipath signal power ratio versus satellite elevation provided in [19], [20] for the Inmarsat system, a Rice's factor $\alpha = 14.5$ dB can be obtained for an average elevation angle $\theta = 19^\circ$.

³The gross bandwidth of 12.5 MHz includes also the guard band introduced through carrier spacing to limit the adjacent-channel interference.

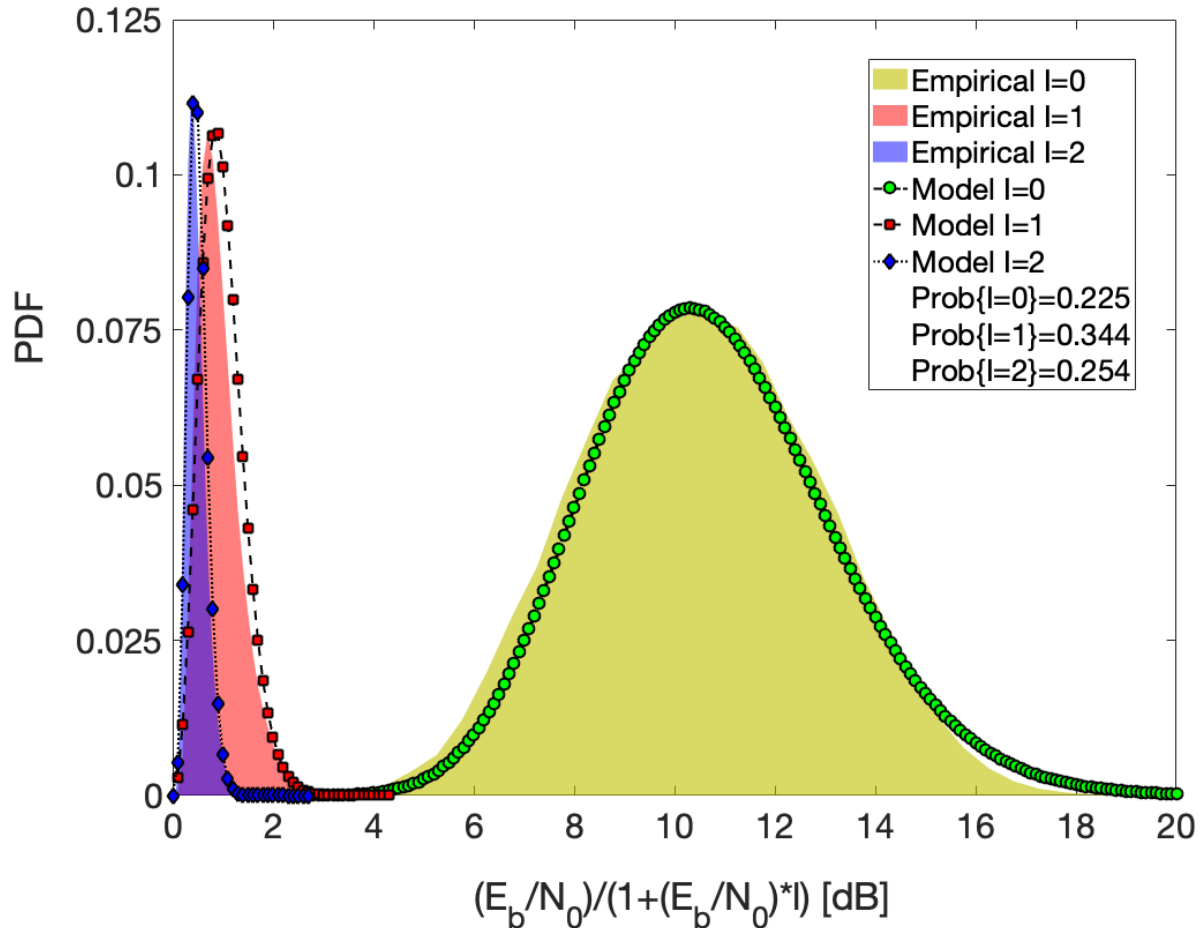


Fig. 1: Example of empirical vs. analytical PDF f_{jI} of the SNIR ($G = 0.5$, $i = \{0;1;2\}g$).

The corresponding delay power profile of the simulated channel exhibits an RMS delay spread $\sigma_{\tau} = 49$ ns and a coherence bandwidth of $B_c = 3.2$ MHz, the latter computed according to $B_c = \frac{1}{2\sigma_{\tau}}$. The channel coherence time can be approximated as $T_c = \frac{1}{f_c \frac{v \cos(\theta)}{c}}$, yielding $T_c = 2.6$ ms for a carrier frequency $f_c = 29.5$ GHz and an average speed of the mobile terminal $v = 15$ Km/h, as then used in our simulations.

Figure 1 shows $f_{jI}(jI)$ at the receiver for $i = \{0;1;2\}g$ interfering packets with the PoI, at load $G = 0.5$ (i.e., 32 users experiencing Rician fading and transmitting in a frame composed of 64 time slots). The plotted areas represent the empirical distributions of $f_{jI}(jI)$ obtained by simulations, while the dotted lines with markers are the relative analytical curves. Finally, the values of the probabilities of having $i = 0:::2$ interfering packets, derived from simulations, are reported in the legend of the plot. In fact, if $i > 2$, a packet could be decoded either thanks

to a spreading factor $S_f > 1$ (this is not the case of this paper), or through IC, as addressed in this paper and further discussed in Section II-B.

B. Numerical Results

The modulation and coding scheme, used in the simulations, account for a QPSK mapping scheme with Forward Error Correction (FEC) code rate 1/2. Yet, each user can transmit a number of replicas $k = 2;3$ over a frame of $n = 64$ time slots.

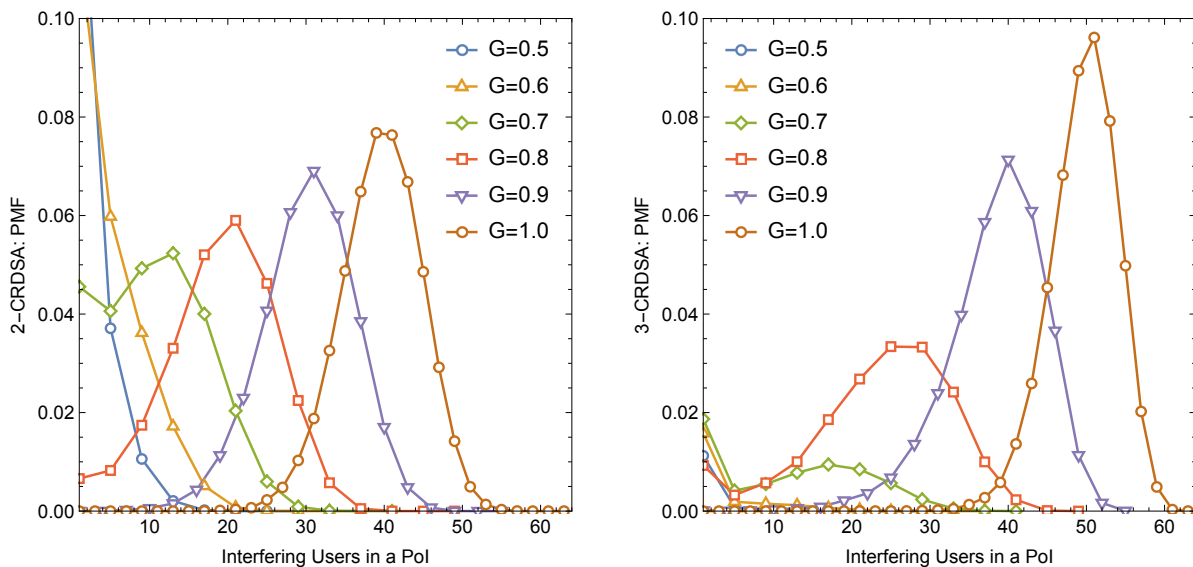


Fig. 2: Empirical distributions of the number of interfering users in a PoI $l = 1 \dots 63$ for $G = 0.5 \dots 1.0$ in 2- and 3-CRDSA with Rice fading.

We focused our analysis in a significant range of normalized traffic load G between 0.5 and 1.0, being $G = U/N$ the number of transmitting user per slot in each frame. Figure 2 shows the empirical Probability Mass Function (PMF) $P_{loop}(l)$ of the number of users interfering with a PoI for values of G simulated on S-NS3, in the range mentioned before, for both 2- and 3-CRDSA. With $G < 0.5$, loop events become rare and the analysis is not significant. However, it has been well demonstrated in literature that a random access scheme like CRDSA performs almost ideally with $PLR = 0$. In fact, PLR models in [13], [14] fit accurately the simulations up to $G = 0.6$.

However, if $G > 0.6$ and, more generally, using more than 2 replicas, the model in [13] provides a not negligible error as discussed in [12].

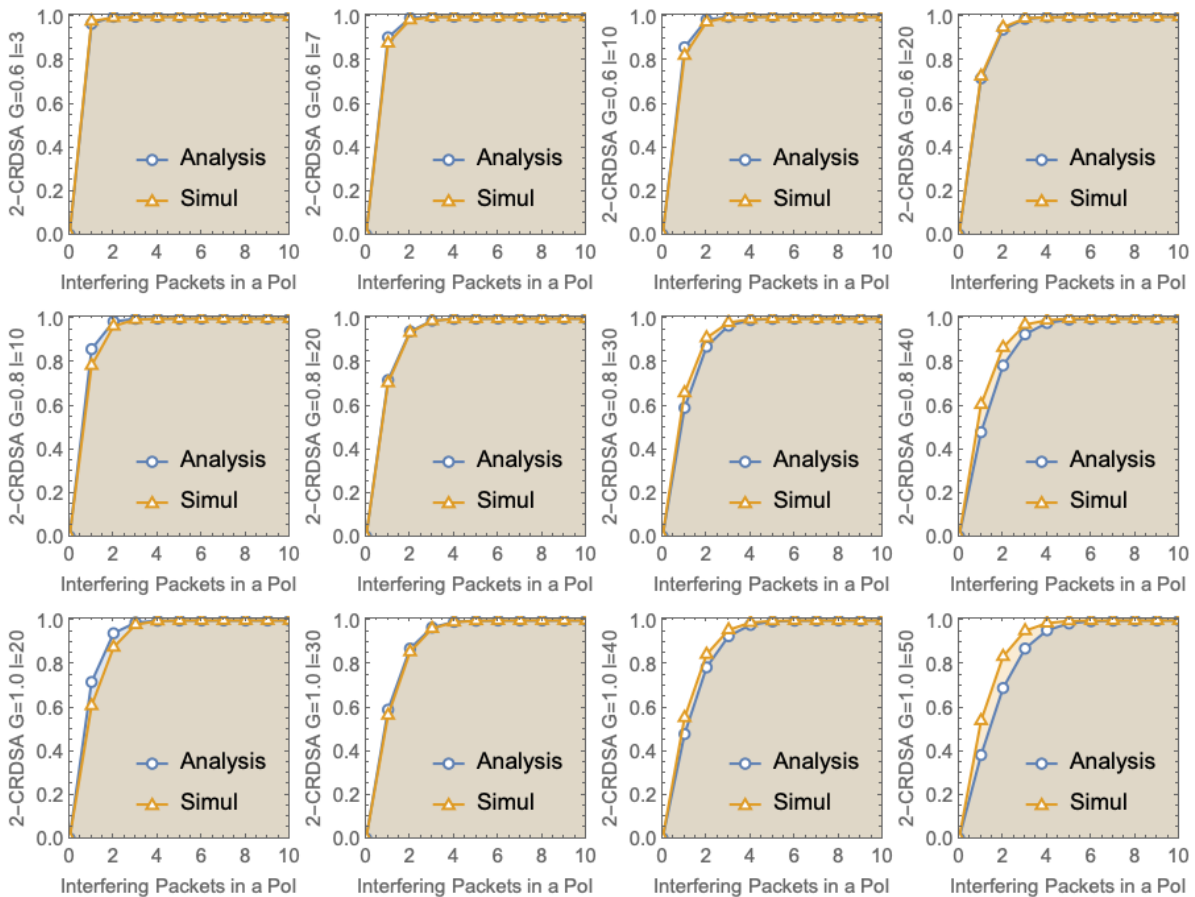


Fig. 3: Analytical Vs. empirical CDF $F_{l|L}$ of the number of interfering packets l with a packet in a PoI in l -order loop for 2-CRDSA at different normalized load $G = 0.6; 0.8; 1.0$

Figure 3 and 4 show the CDFs $F_{l|L}$ for 2- and 3-CRDSA, by comparing (4) with the empiric distribution derived from the simulation campaign with S-NS3.

Table IV and V show the average number of packets $E[l|L]$ interfering with PoI in a loop of order l over a pool $L_{l+1} = \{t_1, \dots, t_j, g\}$ of time slots for 2- and 3-CRDSA, respectively. The number of interfering user l can assume the values in the first column of the two tables with probabilities that can be read in the PMFs in Fig. 2. When $l = 1$, only a single packet can interfere with a PoI. Such an event occurs with a probability that decreases with G . For $G > 0.8$, the probability of having $l = 1$ is almost zero [27]. Again, Eq. (1) assumes that l users in a loop draw the same k -tuple of the PoI in a frame. When this occurs, the number of mutually interfering packets in one of the k time slots is exactly $l + 1$. For example, let us consider the event with 61 users in a loop at $G = 1$ and $k = 3$: it would occur with a probability in the order of 10^{-199}

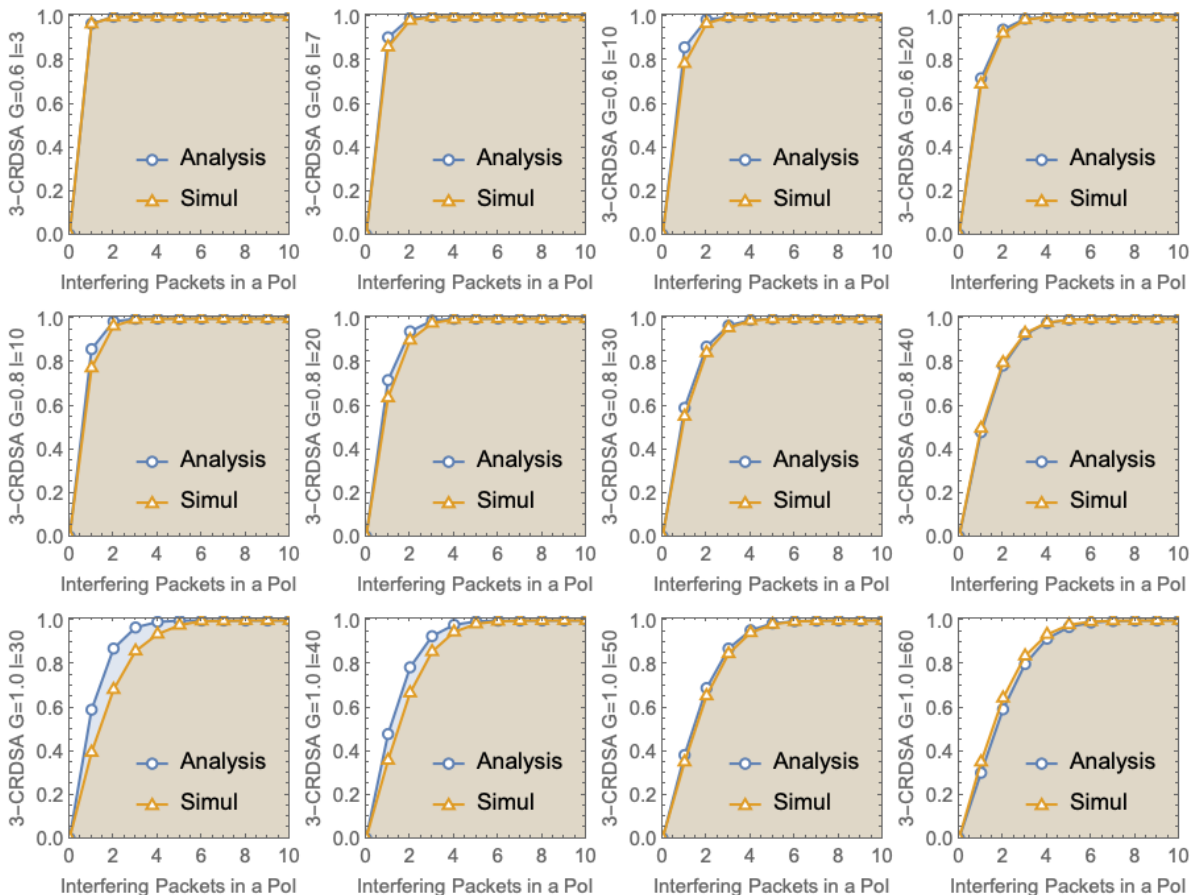


Fig. 4: Analytical Vs. empirical CDF $F_{I|L}$ of the number of interfering packets I with a packet in a PoI in l -order loop for 3-CRDSA at different normalized load $G = 0.6; 0.8; 1.0$

according to Eq. (1). Contrarily, Table V shows that *only* 1:26 packets on average interfere with a PoI and the event has a probability 10^{-4} as in Fig. 2: the pool of slots in the loop is $(61 - 3) = (1 + 2 \cdot 26) = 56$. In fact, only eight slots (64-56) are not in the pool of those in loop. It is worth noting that having 3 users (out of 64, i.e., $G = 1$) not in the loop requires 5 to 9 time slots not in the loop, as exemplified in Table VI.

Finally, Figure 5 shows the resulting PLR for 2- and 3-CRDSA by comparing: (i) the simulation results; (ii) PLR in [13]; (iii) $\hat{P}LR$ calculated by exploiting Eq. (5). Figure 5 takes into account a range of normalized offered loads around realistic system working points identified in [28], [29].

We remark that 2-CRDSA provides a slightly better performance at $G = 1$ than 3-CRDSA as confirmed both by the proposed analytical framework and by the simulation results. This is also

TABLE IV: Average value of the number of interfering packets $E[I|jL]$ with a packet in a PoI for a l -order loop for 2-CRDSA.

| l | $E[I jL]$ | | | | | |
|-----|-----------|---------|---------|---------|---------|---------|
| | $G=0.5$ | $G=0.6$ | $G=0.7$ | $G=0.8$ | $G=0.9$ | $G=1.0$ |
| 1 | 1 | 1 | 1 | 1 | - | - |
| 3 | 1.02 | 1.02 | 1.03 | 1.04 | - | - |
| 5 | 1.08 | 1.08 | 1.10 | 1.12 | - | - |
| 7 | 1.13 | 1.14 | 1.16 | 1.20 | 1.24 | - |
| 10 | 1.18 | 1.20 | 1.22 | 1.25 | 1.35 | - |
| 20 | - | 1.33 | 1.33 | 1.37 | 1.44 | 1.54 |
| 30 | - | - | 1.40 | 1.45 | 1.52 | 1.63 |
| 40 | - | - | - | 1.56 | 1.57 | 1.66 |
| 50 | - | - | - | - | 1.68 | 1.69 |
| 60 | - | - | - | - | - | - |

TABLE V: Average value of the number of interfering packets $E[I|jL]$ with a packet in a PoI for a l -order loop for 3-CRDSA.

| l | $E[I jL]$ | | | | | |
|-----|-----------|---------|---------|---------|---------|---------|
| | $G=0.5$ | $G=0.6$ | $G=0.7$ | $G=0.8$ | $G=0.9$ | $G=1.0$ |
| 1 | 1 | 1 | 1 | - | - | - |
| 3 | 1.02 | 1.03 | 1.08 | - | - | - |
| 5 | 1.10 | 1.10 | 1.14 | 1.15 | 1.25 | - |
| 7 | 1.16 | 1.19 | 1.19 | 1.22 | 1.29 | - |
| 10 | 1.16 | 1.22 | 1.23 | 1.28 | 1.48 | - |
| 20 | - | 1.39 | 1.42 | 1.47 | 1.64 | - |
| 30 | - | - | 1.58 | 1.65 | 1.83 | 2.15 |
| 40 | - | - | - | 1.78 | 1.94 | 2.18 |
| 50 | - | - | - | - | 2.00 | 2.22 |
| 60 | - | - | - | - | - | 2.26 |

evident looking at both the PMFs of the number of interfering users in Fig. 2, and at the average number of interfering packets in tables IV and V, with always more than 2 interfering packets in a PoI with $G = 1$ at any loop order l . Anyway, 3-CRDSA provides better performance in terms of throughput w.r.t. 2-CRDSA or IRSA [30] with frame sizes between 64 and 128 time slots. Moreover, if congestion control algorithms are operated by the upper layer protocols (i.e, transport layer), it turns out that the working points are subject to PLR close to 10^{-3} and to

TABLE VI: Example of the minimum number of time slots ($t_i = 5$) in order to allocate $u_j = 3$ users without loops.

| | t_1 | t_2 | t_3 | t_4 | t_5 |
|-------|-------|-------|-------|-------|-------|
| u_1 | o | | | o | o |
| u_2 | | o | | o | o |
| u_3 | | | o | o | o |

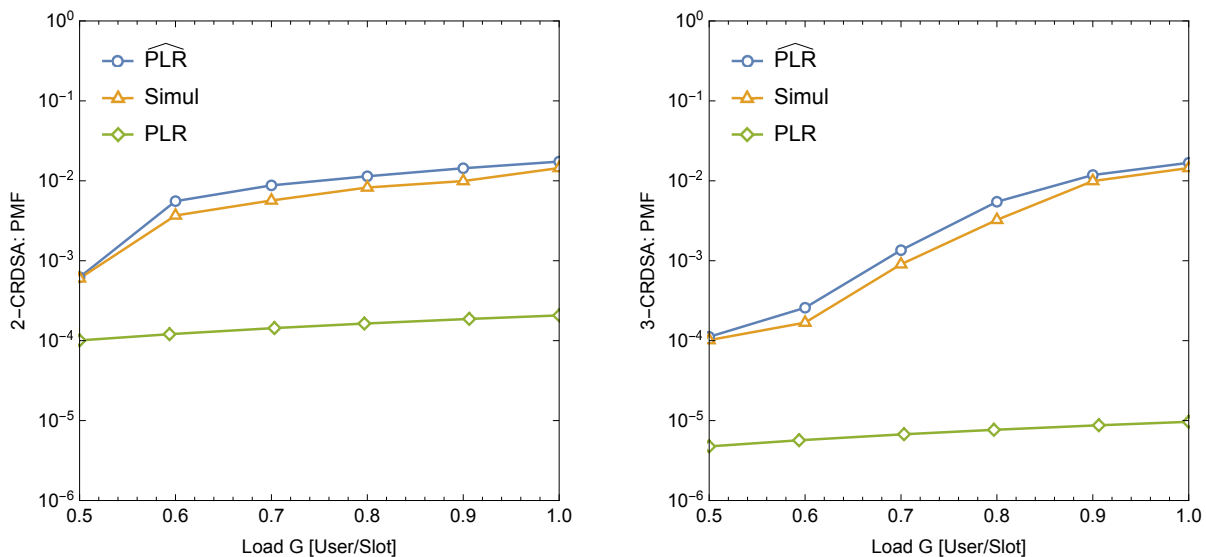


Fig. 5: PLR of 2- and 3-CRDSA with Rice fading: S-NS3 simulations vs. PLR in [5] vs. novel statistical analysis $\widehat{\text{PLR}}$.

10^{-2} , for Transmission Control Protocol (TCP) [28] and TCP Friendly Rate Control (TFRC)-like [29] respectively, when 3-CRDSA is in use, i.e., 3-CRDSA will never pull G over 0.8 with a congestion control in use.

It must be noted that the proposed framework could be adopted also with irregular repetitions of replicas, like IRSA, by exploiting the proper column margins and the relative probabilities, which would occur with.

IV. CONCLUSIONS

This paper propose a novel and accurate framework of analysis of D-FSA schemes with IC for random access satellite platforms, such as CRDSA. To this end, advanced analytical frameworks

and suitable simulation tools have been adopted for carrying out the performance evaluation, by taking, as reference, some recent scientific works on this subject. Particular attention has been devoted to the existing analytical models and simulation results of the literature, deriving the difficulty to correctly estimate the loop probability and the resulting PLR in a D-FSA system. To take these important aspects into consideration, this paper has provided a deep and complete statistical analysis on loop events, the distribution of packets, and of users in a loop, and how they can be combined in frames with the presence of loops, eventually proposing a theoretical framework. Closed forms of the probability distribution functions are obtained fostering on a mathematical framework to count the number of all the binary matrices with prescribed columns and rows, which account for all the possible manifestations of a given number of user U over n time slots in a frame with k attempts each. The performance evaluation shows the accuracy of the model in many significant cases with two different configurations: 2- and 3-CRDSA.

ACKNOWLEDGMENTS

The authors would like to thank Dr. Marco Colucci for his precious contribution to the simulation campaign.

APPENDIX A

This appendix describes the theoretical framework for deriving the analytical expression for $\rho_{loop}(l)$, i.e., the probability that only l users are in a loop with a PoI, after performing IC operations, given the relevant configuration parameters of CRDSA, i.e. n , u , and k .

A. Binary Matrix with prescribed row and column Margin

Let the *column margin* $\mathcal{C} = (c_1; c_2; \dots; c_n) \in \mathbb{N}^n$ be an ordered vector and $h_{\mathcal{C}}(z) := \sum_{c \in \mathcal{C}} z^c$ the set of the whole vectors, whose elements sum to Z , i.e, which is given by all the possible unique permutations c of the c_i parts of each ordered vector \mathcal{C} , such that:

$$c = (m_1; m_2; \dots; m_s)$$

with $m_1; m_2; \dots; m_s$ the multiplicities of the c_i parts. Analogously, let the *row margin* $\mathcal{R} = (r_1; r_2; \dots; r_u) \in \mathbb{N}^u$ be the vector with $r_j = k$, which accounts for the k replicas transmitted by each user u_j . Note that $h_{\mathcal{R}}(z) = z^{\mathcal{R}}$ for CRDSA with k constant replicas and r_j is trivially 1. Then, let's consider the set $\mathcal{M}_{h_{\mathcal{C}}; h_{\mathcal{R}}}(z)$ of binary matrices with $h_{\mathcal{C}}$ columns and \mathcal{R} row such that

the total number of elements (ones) of each binary matrix $\mathcal{M}_{\mathcal{H}c_i \tau}$ is equal to z . Therefore, for u users (rows) and k replicas, it stands that:

$$\prod_{i=1}^u c_i = \prod_{j=1}^k r_j = k \quad u:$$

The set $\mathcal{M}_{\mathcal{H}c_i \tau}(k \quad u)$ accounts for all the possible manifestations of u users transmitting k replicas over a frame of n time slots and its cardinality $j \quad j$ can be calculated by:

$$|\mathcal{M}_{\mathcal{H}c_i \tau}(k \quad u)| = \frac{n!}{k^u} \quad (8)$$

B. Counting Binary Matrices

Let $\mathcal{M}_{\mathcal{C} \tau}$ be the set of binary matrices with prescribed column and row vectors \mathcal{C} and \mathcal{T} , respectively. The cardinality $N(\mathcal{T}; \mathcal{C}) = |\mathcal{M}_{\mathcal{C} \tau}|$ is recursively calculated in [31] as:

$$N(\mathcal{T}; \mathcal{C}) = \prod_{\mathcal{S} \subseteq \mathcal{H}c(z)} \frac{|\mathcal{C}|}{|\mathcal{S}|} N(L\mathcal{T}; \mathcal{C} \cap \mathcal{S}); \quad (9)$$

with L denotes the left-shift map $L\mathcal{T} = (r_2; r_3; \dots)$, $\mathcal{C} \cap \mathcal{S} := \mathcal{C} \setminus \mathcal{S} + L\mathcal{S}$, which can be read as \mathcal{C} reduce \mathcal{S} , and $\begin{matrix} \mathcal{C} \\ \mathcal{S} \end{matrix} := \begin{matrix} \mathcal{C}_1 & \mathcal{S} & \mathcal{C}_1 & \mathcal{S} \\ s_1 & & s_1 & \end{matrix} \quad \begin{matrix} \mathcal{C}_n \\ \mathcal{S} \end{matrix}$.

Therefore, the probability $P_{\mathcal{C} \tau}$ is given by (8) and (9) as:

$$P_{\mathcal{C} \tau}(u; n; k) = \frac{N(\mathcal{T}; \mathcal{C})}{\frac{n!}{k^u}} \quad (10)$$

C. Column margins for users in loop and not

Let's consider l users in loop with a PoI such that $l + 1$ users shares the same set of time slots with their replicas, then set of column margins $\mathcal{H}c_i^{(l+1)}$, allowed by our counting problem, contains the column margins that generate exactly $l + 1$ users in loops and that use $k \quad n$ time slots, once the IC process is completed. Hence, we are looking for the set of column margins

$$\mathcal{H}c_i^{(l+1)}((l + 1)k) := \mathcal{H}c^{(l+1)} \subseteq \mathbb{N}^n : \prod_{i=1}^n c_i^{(l+1)} = (l + 1)kg; \quad (11)$$

which generates the set of binary matrices $\mathcal{M}_{\mathcal{H}c_i^{(l+1)} \tau}$.

The elements in $\mathcal{H}c_i^{(l+1)}$ can be evaluated, by assuming that each margin is composed by two sub-margins $\mathcal{H}c_i^{(l+1)}_L$ and $\mathcal{H}c_i^{(l+1)}_{NL}$, respectively. The first one counts the number of replicas per time slot of the users in loop and the second one counts the number of replicas per time slot of the users not in loop, i.e, those resolved by IC. The set $\mathcal{H}c_i^{(l+1)}_L$ is obtained by the integer partition of the number of replicas $(l + 1)k$ in $[k; b(l + 1)k=2c]$ integers, where the integers

range in $[2; l + 1]$. The set $h\mathcal{C}_{NL}^{(l+1)}$ is obtained by the integer partition of the number of replicas $(u - l - 1)k$ in $[k; n]$ integers, where the integers range in $[1; u - l - 1]$, and then by filtering this set, as explained in the following. We assume that $h\mathcal{C}_{NL}^{(l+1)} \ni \mathcal{C}_{NL}^{(l+1)} = (h_{a_2 l}; h_{a_1 l}; h_{a_0 l})$, where $h_{a_2 l}; h_{a_1 l}; h_{a_0 l}$ are the sets of elements in the column margin greater than 1, equal to 1, and equal to 0, respectively. The column margin can be selected, whether the number of users in loop at the end of IC steps is $l + 1$: this can occur only by removing the replicas of the users that have at least a replica alone in a time slot. This means that the number of time slots

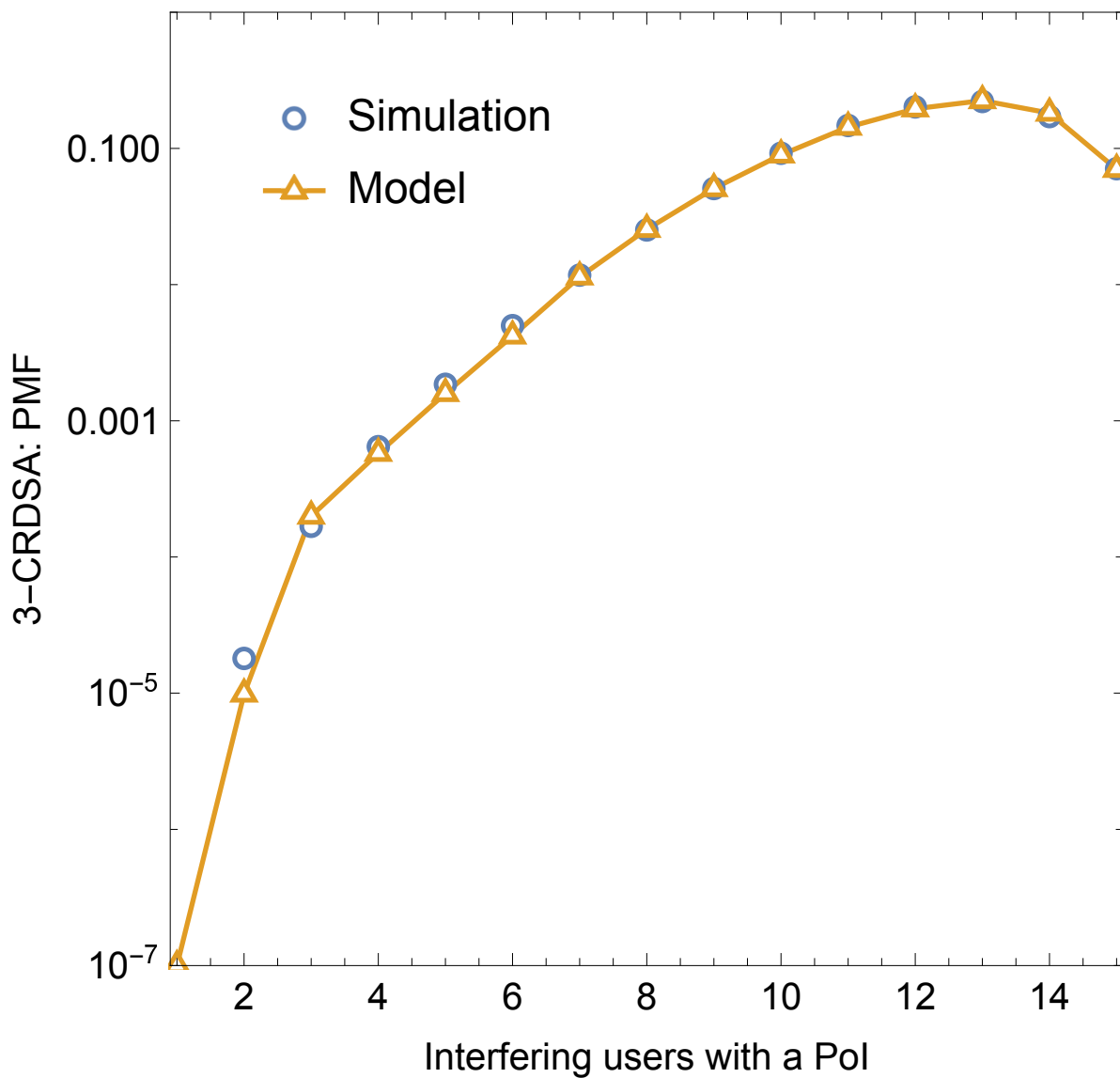


Fig. 6: Analytical Vs. empirical PMF $\rho_{loop}(l)$ of the number of interfering users l with a packet in a PoI in l -order loop for 3-CRDSA

must be large enough to contain at each step of IC the number of integers needed to partition the number of replicas of the users not in loop minus the replicas of users not in loop with at least one replica alone in a time slot, assuming the integers of the partition strictly equal to 2. Formally, such a condition can be stated as follows: the number of available time slots $n^0 = jha_{2ij} + \max[0; jha_{2ij} - (u - l - 1)]$ must be greater than or equal to the number of needed time slots

$$n^0 = \frac{\sum_{i=1}^6 P_{jha_{2ij}} a_{2;i} - \sum_{i=1}^7 jha_{1ij}(k - 1)}{2} + 1.$$

The elements in $h_{ci}_L^{(l+1)}$ and $h_{ci}_{NL}^{(l+1)}$ have to be combined so that the resulting column margins $h_{ci}^{(l+1)} \in \mathcal{C}^{(l+1)} = (hb_{2i}; hb_{1i}; hb_{0i})$ satisfy the conditions stated below, assuming that $hb_{2i}; hb_{1i}; hb_{0i}$ are the sets of elements in the column margin greater than 1, equal to 1, and equal to 0, respectively.

The filtering rules for the column margins $\mathcal{C}^{(l+1)}$ are:

If $jhb_{1ij} \geq u - l - 1$, the integer partition of jhb_{1ij} in $u - l - 1$ integers can be calculated with integers less or equal to k , and, for the column margins that satisfy this constraint, only the number of matrices, which allow exactly $u - l - 1$ transmitting users, have to be taken in to account: further details are provided in [32].

If $jhb_{1ij} < u - l - 1$, given $n^{000} = jhb_{2ij} + jhb_{1ij}$ the number of elements in the column margin greater than zero, the difference $c_{i+1}^{(l+1)} - c_i^{(l+1)} \geq n^{000}$ has to be less or equal to 1.

D. Loop probability

The loop probability function $P_{loop}(l) = P(l; u; n; k)$ can be obtained by combining (10) with (11) as:

$$P(l; u; n; k) = \frac{u!}{(l+1)!} \times \prod_{j \in \mathcal{C}^{(l+1)}} P_j \tau(u; n; k) \quad (12)$$

Figure 6 shows the perfect match between analysis and simulation in a simple test case with $u = 16$, $n = 16$, $k = 3$, equivalent to a system load $G = 1$.

REFERENCES

- [1] A. Davies, "Satellite IoT Forecast 2019-2025," 2019. [Online]. Available: <http://tinyurl.com/y32s68qs>
- [2] R. De Gaudenzi, O. Del Rio Herrero, G. Gallinaro, S. Cioni, and P.-D. Arapoglou, "Random access schemes for satellite networks, from vsat to m2m: a survey," *International Journal of Satellite Communications and Networking*, vol. 36, no. 1, pp. 66–107, 2018.

- [3] S. Cioni, R. De Gaudenzi, O. Del Rio Herrero, and N. Girault, "On the satellite role in the era of 5g massive machine type communications," *IEEE Network*, vol. 32, no. 5, pp. 54–61, Sep. 2018.
- [4] A. Guidotti, A. Vanelli-Coralli, M. Conti, S. Andrenacci, S. Chatzinotas, N. Maturo, B. Evans, A. Awoseyila, A. Ugolini, T. Foggi, L. Gaudio, N. Alagha, and S. Cioni, "Architectures and key technical challenges for 5g systems incorporating satellites," *IEEE Transactions on Vehicular Technology*, vol. 68, no. 3, pp. 2624–2639, March 2019.
- [5] O. D. R. Herrero and R. De Gaudenzi, "High Efficiency Satellite Multiple Access Scheme for Machine-to-Machine Communications," *IEEE Transactions on Aerospace and Electronic Systems*, vol. 48, no. 4, pp. 2961–2989, 2012.
- [6] N. Celandroni, E. Ferro, and A. Gotta, "RA and DA satellite access schemes: a survey and some research results and challenges," *International Journal of Communication Systems*, vol. 27, no. 11, pp. 2670–2690, 2014.
- [7] N. Celandroni and R. Secchi, "Suitability of DAMA and Contention-Based Satellite Access Schemes for TCP Traffic in Mobile DVB-RCS," *IEEE Transactions on Vehicular Technology*, vol. 58, no. 4, pp. 1836–1845, May 2009.
- [8] E. Casini, R. D. Gaudenzi, and O. Herrero, "Contention Resolution Diversity Slotted ALOHA (CRDSA): An Enhanced Random Access Scheme for Satellite Access Packet Networks," *IEEE Transactions on Wireless Communications*, vol. 6, no. 4, pp. 1408–1419, 2007.
- [9] G. Liva, "Graph-Based Analysis and Optimization of Contention Resolution Diversity Slotted ALOHA," *IEEE Transactions on Communications*, vol. 59, no. 2, pp. 477–487, February 2011.
- [10] C. Stefanovic, E. Paolini, and G. Liva, "Asymptotic Performance of Coded Slotted ALOHA With Multipacket Reception," *IEEE Communications Letters*, vol. 22, no. 1, pp. 105–108, Jan 2018.
- [11] C. H. Wei, R. G. Cheng, and S. L. Tsao, "Modeling and Estimation of One-Shot Random Access for Finite-User Multichannel Slotted ALOHA Systems," *IEEE Communications Letters*, vol. 16, no. 8, pp. 1196–1199, August 2012.
- [12] M. Bacco, P. Cassarà, A. Gotta, and T. de Cola, "Diversity framed slotted aloha with interference cancellation for maritime satellite communications," in *2019 IEEE International Conference on Communications (ICC)*. IEEE, 2019, pp. 1–6.
- [13] O. del Rio Herrero and R. De Gaudenzi, "Generalized Analytical Framework for the Performance Assessment of Slotted Random Access Protocols," *IEEE Transactions on Wireless Communications*, vol. 13, no. 2, pp. 809–821, 2014.
- [14] A. Mengali, R. De Gaudenzi, and P.-D. Arapoglou, "Enhancing the Physical Layer of Contention Resolution Diversity Slotted ALOHA," *IEEE Trans. Commun*, vol. 65, no. 10, pp. 4295–4308, 2017.
- [15] F. Baccelli and B. Blaszczyszyn, "Stochastic Geometry and Wireless Networks, Volume I (theory)," *Foundations and Trends in Networking*, vol. 3, no. 3-4, pp. 249–449, 2009.
- [16] —, "Stochastic Geometry and Wireless Networks, Volume II (applications)," *Foundations and Trends in Networking*, vol. 4, no. 1-2, pp. 1–312, 2009.
- [17] H. A. Ammar, Y. Nasser, and H. Artail, "Closed Form Expressions for the Probability Density Function of the Interference Power in PPP Networks," in *2018 IEEE International Conference on Communications (ICC)*. IEEE, 2018, pp. 1–6.
- [18] Z. Hijaz, V. S. Frost, and B. Davis, "Probability Density Function of SINR in Nakagami-m Fading with Different Channels," in *Information and Telecommunication Technology Center Kansas University Technical Report*. Kansas University, 2013, pp. 1–5.
- [19] J. Hagenauer, F. Dolainsky, E. Lutz, W. Papke, and R. Schweikert, "The Maritime Satellite Communication Channel-Model, Performance of Modulation and Coding," *IEEE Journal on Selected Areas in Communications*, vol. 5, no. 4, pp. 701–707, 1987.
- [20] E. Lutz, D. Cygan, M. Dippold, F. Dolainsky, , and W. Papke, "The Land Mobile Satellite Communication Channel-Recording, Statistics, and Channel Model," *IEEE Transaction on Vehicular Technology*, vol. 40, no. 2, pp. 375–386, 1991.
- [21] A. R. Miller, R. M. Brown, and E. Vegh, "New derivation for the rough surface reflection coefficient and for distribution of sea-wave elevations," *Microwaves, Optics and Antennas, IEE Proceedings H*, vol. 131, no. 1, pp. 114–116, 1984.

- [22] K. An, T. Liang, G. Zheng, X. Yan, Y. Li, and S. Chatzinotas, "Performance limits of cognitive-uplink FSS and terrestrial FS for Ka-band," *IEEE Transactions on Aerospace and Electronic Systems*, vol. 55, no. 5, pp. 2604–2611, 2018.
- [23] W. Lu, K. An, and T. Liang, "Robust beamforming design for sum secrecy rate maximization in multibeam satellite systems," *IEEE Transactions on Aerospace and Electronic Systems*, vol. 55, no. 3, pp. 1568–1572, 2019.
- [24] Q. Huang, M. Lin, W.-P. Zhu, S. Chatzinotas, and M.-S. Alouini, "Performance analysis of integrated satellite-terrestrial multiantenna relay networks with multiuser scheduling," *IEEE Transactions on Aerospace and Electronic Systems*, 2019.
- [25] J. Puttonen, S. Rantanen, F. Laakso, J. Kurjenniemi, K. Aho, and G. Acar, "Satellite model for Network Simulator 3," in *Proceedings of the 7th International ICST Conference on Simulation Tools and Techniques*. ICST (Institute for Computer Sciences, Social-Informatics and Telecommunications Engineering), 2014, pp. 86–91.
- [26] ETSI, "Digital Video Broadcasting (DVB); second generation DVB interactive satellite system (DVB-RCS2); part 2: Lower layers for satellite standard, ETSI EN 301 545–2 V1.2.1," Standard, Apr. 2014.
- [27] M. Bacco, P. Cassarà, E. Ferro, and A. Gotta, "Generalized Encoding CRDSA: Maximizing Throughput in Enhanced Random Access Schemes for Satellite," in *International Conference on Personal Satellite Services*. Springer, 2013, pp. 115–122.
- [28] M. Bacco, T. De Cola, G. Giambene, and A. Gotta, "TCP-Based M2M Traffic via Random-Access Satellite Links: Throughput Estimation," *IEEE Transactions on Aerospace and Electronic Systems*, vol. 55, no. 2, pp. 846–863, April 2019.
- [29] M. Bacco, P. Cassarà, M. Colucci, and A. Gotta, "Modeling Reliable M2M/IoT Traffic Over Random Access Satellite Links in Non-Saturated Conditions," *IEEE Journal on Selected Areas in Communications*, vol. 36, no. 5, pp. 1042–1051, May 2018.
- [30] N. Celandroni, F. Davoli, E. Ferro, and A. Gotta, "On Elastic Traffic via Contention Resolution Diversity Slotted Aloha Satellite Access," *International Journal of Communication Systems*, vol. 29, no. 3, pp. 522–534, 2016.
- [31] J. Miller and M. Harrison, "Exact sampling and counting for fixed-margin matrices," *Annals of Statistics*, vol. 41, no. 3, pp. 1569–1592, 2013.
- [32] P. Cassarà, M. Colucci, and A. Gotta, "Command and Control of UAV Swarms via Satellite," *Springer, Lecture Notes of the Institute for Computer Sciences, Social Informatics and Telecommunications Engineering*, vol. 231, pp. 86–95, March 2018.



Pietro Cassarà received his M.Sc. degrees in Telecommunication and Electronic Engineering from University of Palermo in the 2005, and its Ph.D. degree in the 2010, jointly with the State University of New York. Nowadays, he is staff member of the Institute of Science and Information Technologies (ISTI), at the National Research Council (CNR), Pisa, Italy, and since 2017 he is temporary staff member of the CMRE lab at the NATO of La Spezia. His research interests include learning and stochastic control for wireless sensor network and IoT communications. He has been participating in European-funded and National-funded projects.

National-funded projects.

